EUROPEAN ORGANIZATION FOR NUCLEAR RESEARCH

CERN–EP/90–26
22 February 1990

LIFETIME MEASUREMENTS OF THE D^+, D^0, D_s^+, AND Λ_c^+ CHARMED PARTICLES

M.P. Alvarez[2], R. Barate[3b], D. Bloch[9], P. Bonamy[7], P. Borgeaud[7], M. Burchell[4], H. Burmeister[3], J.M. Brunet[6], F. Calvino[2a], M. Cattaneo[4], J.M. Crespo[2], B. d'Almagne[5], M. David[7], L. DiCiaccio[3c], J. Dixon[4], P. Druet[5], A. Duane[4], J.P. Engel[9], A. Ferrer[3d], T.A. Filippas[1], E. Fokitis[1], R.W. Forty[4], P. Foucault[9], E.N. Gazis[1], J.P. Gerber[9], Y. Giomataris[3], T. Hofmokl[10], E.C. Katsoufis[1], M. Koratzinos[3,4,5], C. Krafft[5], B. Lefievre[6], Y. Lemoigne[7], A. Lopez[3,5*], W.K. Lui[8], C. Magneville[7], A. Maltezos[1], J.G. McEwen[8], Th. Papadopoulou[1], B. Pattison[3], D. Poutot[6], M. Primout[7], H. Rahmani[1], P. Roudeau[5], C. Seez[4], J. Six[5], R. Strub[9], D. Treille[3], P. Triscos[6], G. Tristram[6], G. Villet[7], A. Volte[6], M. Wayne[5], D.M. Websdale[4], G. Wormser[5] and Y. Zolnierowski[3]

(The NA14/2 Collaboration)

(Submitted to Zeitschrift für Physik)

---

1) National Technical University, Athens, Greece.
2) Universidad Autónoma de Barcelona, Bellaterra, Spain.
3) CERN, Geneva, Switzerland.
4) Blackett Lab., Imperial College, London, UK.
5) LAL, IN2P3–CNRS and Univ. Paris-Sud, Orsay, France.
6) Collège de France, Paris, France.
7) DPhPE, CEN–Saclay, Gif-sur-Yvette, France.
8) Univ. of Southampton, Southampton, UK.
9) CRN, IN2P3–CNRS and Univ. L. Pasteur, Strasburg, France.
10) Univ. of Warsaw, Warsaw, Poland.
a) Univ. Politecnica de Catalunya, ETSEIB–DEN, Barcelona, Spain.
b) Univ. J. Fourier and ISN, Grenoble, France.
c) Univ. di Roma II, 'Tor Vergata', Rome, Italy.
d) Univ. de Valencia, IFIC, Valencia, Spain.
*) On leave from Fac. de Ciencias Fisicas, Univ. Complutense, Madrid, Spain.

ABSTRACT

Using a high-statistics sample of more than 1000 reconstructed charmed-particle decays, the lifetimes of the weakly decaying charmed mesons and of the Λ_c^+ baryon have been measured:

$$\tau_{D^+} = 1.03 \pm 0.08 \pm 0.06 \text{ ps}, \qquad \tau_{D^0} = 0.417 \pm 0.018 \pm 0.015 \text{ ps}$$

$$\tau_{D_s^+} = 0.33\ ^{+0.12}_{-0.08}\ \pm 0.03 \text{ ps}, \qquad \tau_{\Lambda_c^+} = 0.18 \pm 0.03 \pm 0.03 \text{ ps}$$

1. INTRODUCTION

Whilst in the Spectator Quark Model the scale of charmed-particle lifetimes is explained by the mass of the charm quark, the large lifetime differences observed between the various charmed states indicate the importance of non-spectator processes in their decay mechanisms. The large D^+ lifetime*) is attributed to a destructive Pauli interference due to the presence of two identical partons in the final state. The small Λ_c^+ lifetime is supposed to come from the contribution of the scattering graph; unlike the corresponding process (usually called the annihilation graph) that contributes also to the D^0 or D_s^+ decays, this scattering graph is not suppressed by helicity conservation.

2. THE NA14/2 EXPERIMENT

The NA14 spectrometer was originally designed to study the photoproduction of photons and hadrons at high transverse momenta [1], and is characterized by a large angular acceptance for such particles. A schematic layout of the present apparatus is shown in Fig. 1.

The experimental photon beam is produced by the bremsstrahlung of electrons, which are generated indirectly from the protons of the CERN Super Proton Synchrotron (SPS). Every 12 s a burst of 8×10^7 electrons is incident, over a period of 2 s, on a 0.1 X_0 thick lead radiator. The resulting photon beam has high luminosity ($\sim 10^7$ per burst, $E_\gamma > 50\,\mathrm{GeV}$) and negligible hadron contamination.

For the study of charm, the chief modification to the apparatus of the previous experiment was the addition of a high-resolution silicon vertex detector. A description of the apparatus and some other details relevant to the current analysis are given below.

Charged particles are deflected by two magnets having a total integrated $B \cdot \ell$ of 4 T·m, and are measured by 73 MWPC planes, leading to a typical mass resolution for a D-meson of $\sigma_M \simeq 13\,\mathrm{MeV}$. An air-filled Cherenkov counter C2 allows the separation of kaons/protons from pions between 6.3 and 20.5 GeV/c and protons from kaons/pions above 21 GeV/c. The upstream Cherenkov counter, C1, filled with Freon is situated in the high magnetic field of the downstream magnet. It has a kaon threshold at 10 GeV/c. To reconstruct neutral particles, three electromagnetic calorimeters are used, two of lead-glass and one of lead/scintillator, covering the geometrical acceptance of the apparatus.

*) Charge conjugate states are implicitly included throughout this paper.

The information from the vertex detector is crucial for reducing the combinatorial background in mass distributions under the charmed particle signals. This detector (Fig. 2) comprises a segmented silicon target with analog readout [2], and a set of 10 planes of 50 μm pitch microstrips, with a large active area of $5 \times 5\,\mathrm{cm}^2$ and digital readout [3].

The silicon active target is segmented along the beam direction in 500 μm steps (300 μm of silicon, 200 μm of air). Each plane of silicon is subdivided into 2.1 mm strips in a plane transverse to the beam. The amplitude of the signals gives a measurement of the ionization deposited around the vertex position in the region of the photon interaction.

The telescope of microstrip planes permits the reconstruction of charged-particle tracks with a transverse accuracy of $\sim 17\,\mu$m at the vertex. The planes are arranged in five pairs, with the strips of each pair oriented orthogonally. The first four pairs are arranged horizontally/vertically, whilst the fifth pair is rotated by $\sim 33°$ to provide matching of projection tracks in space. A minimum-ionizing particle gives a signal with a mean value (i.e. 1 mip) of ~ 14 times the noise fluctuation. The readout discriminator threshold is set to 0.35 mip to ensure that the signal of a track that crosses two strips is still registered. The number of spurious hits generated over the whole detector is about six in a 50 ns gate, and the charge sharing is low; 90% of clusters are single hits. To reduce the readout electronics , each data-acquisition channel was used to read two strips—the connection of the strip pairs was arranged so that aligned hits from a charged track give dispersed hits for the paired channels. The per-plane efficiency of the microstrip detector was measured, under normal operating conditions, to be $\sim 97\,\%$, independent of the track angle (up to 150 mrad).

The importance of the vertex detector for the isolation of charmed-particle signals is illustrated in Fig. 3 for the decay $D^+ \to K^-\pi^+\pi^+$, from a sub-sample of the data. This good background rejection permits the reconstruction of charmed particles with a kaon momentum above the 20 GeV/c threshold of C2; as an example, the number of reconstructed $D^0 \to K^-\pi^+$ decays is doubled, with only $\sim 5\%$ of ambiguous candidates ($K\pi \to \pi K$). In case of such ambiguities, we have kept only one mass combination since each candidate corresponds to a unique vertex position.

2.1 Trigger conditions and data acquisition

The trigger of the experiment is designed to select hadronic interactions of the incident photon beam. Most of the photon interactions in the silicon target are electromagnetic, leading to the production of e^+e^- pairs that are created collinear to the beam. When these pairs pass through the magnetic fields of the spectrometer, they are swept into a horizontal band. The trigger makes use of this feature, and requires at least one charged particle above and one below the horizontal region, using scintillator hodoscopes as illustrated schematically in Fig. 4. A further rejection of pairs is achieved with a target condition requiring at least 2.5 mip of charge deposited in each of the last three planes. Upstream of the target, scintillator counters are used to veto muons that accompany the experimental beam, and to ensure that the incident photon has not converted before reaching the target.

The trigger efficiency is 30% for non-charmed hadronic interactions. For charm events, the efficiency is approximately twice as high because of the greater charged track multiplicity, and because the particles are emitted with a higher mean transverse momentum. Approximately 85% of triggers are hadronic events registered inside the active target.

The incident electron energy is measured before and after radiation. The accuracy in the reconstruction of the radiated energy is about 2 GeV . The efficiency of the tagging spectrometer is 40%, limited by the high intensity of the beam . As we measure only the total radiated energy, a correction was applied to take into account the radiation of several photons. This has been determined using a Monte Carlo simulation.

About 60 events per burst were registered on tape. Over the period 1985–86, a total of 17 million events were recorded.

2.2 Data processing

The events were first passed through a fast algorithm that reconstructs charged tracks using the MWPC information, and identifies kaons. Events of interest for particular lines of analysis were selected, using fast filter algorithms, to give a manageable sample for passing through the complete off-line reconstruction programs. Part of the initial sample, i.e. 4.3 million events, was processed directly through the full reconstruction, using the emulator 'farm' facility at CERN, comprising up to

twelve 3081E emulators [4]. This directly processed data-set (DP) is important for the investigation of filter efficiencies and biases.

In the search for D_s^+ and Λ_c^+ decays, selected events had either two kaons or one kaon and one proton, identified using the Cherenkov C2. These filtered data sets will be referred to as KF and PF.

For the D^0 and D^+ meson analysis, the vertex detector information was used to enrich the charm content of the data. This was achieved by matching the tracks seen in the chambers with the corresponding hits in the microstrips. The active target was used to define the primary vertex position along the beam direction, and matched tracks were extrapolated to this position to define the primary vertex coordinates in the transverse plane. These coordinates were used, in a second pass, to associate unmatched tracks with microstrip information. The charm content of the data was then enhanced by rejecting events for which the tracks were compatible with a single vertex. In this manner $\sim 18\%$ of the recorded events were kept, to be passed through the full reconstruction. The efficiency of this 'microstrip' filter (MF) for charm interactions was measured to be between 50% and 60%, depending on the charmed particle and its decay channel.

2.3 Charm analysis

The combination of tracks for a given charmed-particle decay is chosen using the Cherenkov information. The decay tracks are required to be reconstructed in the microstrip detector, and are used to find the decay vertex. For $K\pi$ events, the accuracy along the beam direction is about $500\,\mu$m. The trajectory of the candidate charmed particle is then reconstructed, and is used, together with the remaining tracks in the event, to reconstruct the production vertex. Depending on the χ^2 probability of the vertex fit, the least well associated track—which might come from the second charm decay in the event, or be badly reconstructed—is rejected, and the process is iterated.

The charm signals are then extracted by imposing a cut on their proper time or on the separation of the production and decay vertices, applied either to their separation distance along the beam direction, Δx, or to this distance divided by its error σ_x (determined from the errors in the vertices), $N_\sigma = \Delta x/\sigma_x$.

The selection cut used for each charm decay channel is given in Table 1, together with the number of events passing the cut.

3. PROCEDURE FOR LIFETIME MEASUREMENT

A maximum-likelihood method is used to measure the charmed-particle lifetimes. For each event i, the vertex separation cut—used to extract the charm signals—defines the minimum accessible proper time t^i_{min}. The maximum proper time t^i_{max} is determined by the distance between the primary vertex and the first microstrip plane.

The probability distribution is taken as

$$P(t) = (1 - \epsilon_0)P_S(t) + \epsilon_0 P_B(t)\,,$$

normalized to unity between t^i_{min} and t^i_{max}. (The subscripts S and B denote 'signal' and 'background'.) Here ϵ_0 is the ratio of the number of events coming from the background to the total number of events at t=0. This is not the same as the background fraction ϵ that is measured from the mass distribution of the selected events, and an iterative technique is used to determine a value for ϵ_0 that reproduces the measured ϵ.

The probability distributions for $P_S(t)$ and $P_B(t)$ are of the form P(t)=A(t)f(t), where f(t), for the signal, has an exponential dependence convoluted with a Gaussian distribution to take into account the detector resolution. This distribution is normalized to unity for t varying between $-\infty$ and $+\infty$. The function A(t) corrects for variation of the acceptance with the measured proper time and is determined using a Monte Carlo simulation.

3.1 Acceptance studies with the Monte Carlo simulation

Simulated events have been generated in raw data format and passed through the same reconstruction and analysis programs as those used for the real data samples.

In the case of DP processing, for the $D^0 \to K^-\pi^+$ decay channel we have found no evidence of a bias in the lifetime measurement induced by the analysis chain. For the channel $D^+ \to K^-\pi^+\pi^+$, the measured lifetime is slightly smaller by an amount -0.050 ± 0.027 ps than the generated lifetime, and we have corrected for this systematic effect in the quoted value for the D^+ lifetime.

For the MF data sample, another correction has to be added. This is due to a loss of events at large decay lengths. This loss is identified as being due to a cut that eliminates events having at least one track with a large transverse offset—greater than 500 μm—relative to the primary vertex position.This cut affects mainly the reconstructed D^+ sample because of the larger lifetime of this particle. Its effect has been introduced into

the likelihood function using the behaviour of the acceptance function A(t), which was obtained by comparing the number of reconstructed and generated events observed at a fixed decay length. After this correction on Monte Carlo generated events, we have verified that we recover the lifetime value used in the simulation. The effect of this correction on the lifetime determination is large for D^+ mesons ($\sim$ 30%) and is very small for D^0 decays ($\sim$ 5%).

The uncertainties that affect the determination of the acceptance curve contribute as a systematic error in the lifetime measurement. For events not selected when using the MF algorithm, this uncertainty is dominated by the statistical accuracy of the Monte Carlo generation, which was chosen to be always better than the one for the data. For the MF data sample, we have also to take into account the uncertainties affecting the shape of the acceptance function.

3.2 Effect of the background present under the D signals

To measure the lifetime and the number of events coming from background under the charmed signals, we have used events from the wings in mass distributions as shown in Fig. 5 as an example.

We parametrized the time distribution of events from background with three components. Two of them are taken as exponential distributions. A very steeply falling distribution with effective lifetime $\tau_1 \sim 0.1$ ps is present in samples selected using a small separation between the primary and the decay vertices. It comes from the finite resolution of the detector. A flatter distribution ($\tau_2 \approx 0.3$ ps) accounts for events in which there are tracks from the two charmed particles produced in the event, or from the wrong assignment of hits in the vertex detector. The last component is assumed to be flat and comes from hadronic secondary interactions in the silicon active target.

We have considered that the uncertainties in the background description obtained in this way contribute also as systematic uncertainties in the lifetime determination of charmed particles. These quantities are obtained by looking at the effect, on the lifetime measurement, of a variation by ± 1 standard deviation of the fitted values determined using background events.

A small difference in lifetime determination results from using one or two exponentials for the background description. This is included in the systematic uncertainty.

The fraction of background present in mass distributions is obtained using the sidebands of the signal. The uncertainty in this quantity also contributes as a systematic error in the charm lifetime determination.

4. CHARMED PARTICLE LIFETIMES

We have measured the lifetimes of the D^+, D^0, D_s^+, and Λ_c^+ charmed particles using the signals shown in the effective mass plots presented in Figs. 5a to 9a; the results are summarized in Table 2. The details that are relevant to each channel are given below.

Statistical uncertainties dominate the determination of Λ_c^+ and D_s^+ lifetimes. Attention has to be devoted to the evaluation of systematic errors for D^0 and D^+.

The measured lifetimes of the charmed signals, with background and acceptance corrections, are stable, within the measurement accuracies, for a range of vertex separation cuts in Δ x and N_σ.

For each proper-time distribution (Figs. 5b to 9b) we show as a full line the fitted time evolution for events selected in the mass region of the signal. The corresponding behaviour for events coming from the background under the charm signal is shown as a dashed line.

4.1 D^+ lifetime (Fig. 5)

The D^+ is observed through its $K^-\pi^+\pi^+$ decay mode. We have used only the DP data sample. The MF sample gives similar results but with a larger systematic uncertainty due to the corrections needed to account for the decrease in acceptance at long decay lengths.

4.2 D^0 lifetime (Figs. 6 and 7)

The D^0 signals used for the lifetime measurement are taken from the $K^-\pi^+$ (Fig. 6) and $K^-\pi^+\pi^+\pi^-$ (Fig. 7) decay channels extracted from the MF sample.

For D^0 decays , the uncertainties affecting the level and the shape of the time evolution of background events have only a small influence on the determination of the lifetime of the signal. This is because the mean lifetime of background events is, apart from the steeply falling term, quite similar to the D^0 lifetime.

We have combined the three measurements given in Table 2, taking into account the fact that some events are common to DP and MF data sets.

4.3 D_s^+ lifetime (Fig. 8)

Events are selected in the $\phi\pi^+$ decay mode, using the KF data sample. Two well-separated peaks appear in the mass distribution, corresponding to the D^+ and D_s^+ decays. The D_s^+ signal is defined from the mass distribution, taking events that have mass within 25 MeV/c^2 of the D_s^+ mass. More details concerning the D_s^+ analysis can be found in Ref. [5].

A potential source of systematic error for this measurement is the presence of reflections from other channels, i.e. the contamination of the signal by particles of a different type, which have been reconstructed with the D_s^+ mass owing to misidentification of their decay products. The two most likely candidates are $\Lambda_c^+ \rightarrow pK^-\pi^+$ and $D^+ \rightarrow K^-\pi^+\pi^+$. The masses of the events used for the lifetime measurement were recalculated, taking each of the above reflection hypotheses in turn. Events that were then found to lie within the Λ_c^+ or D^+ mass ranges were excluded, and the lifetime was recalculated, giving an insignificant change of 0.01 ps.

4.4 Λ_c^+ lifetime (Fig. 9)

The Λ_c^+ baryon is isolated by using its decay into the $pK^-\pi^+$ channel. The proton and kaon particles are identified by the Cherenkov counter. A detailed description of the algorithm used to extract the signal of the Λ_c^+ particle is given in Ref. [6].

Transforming the proton into a kaon or into a pion, we have searched for a possible contamination of the Λ_c^+ sample by D_s^+ or D^+ decays. No accumulation is seen at the corresponding masses, and only three events have masses compatible with two hypotheses. If these events are removed, the variation of 0.01 ps in the lifetime measurement is negligible in comparison with the other sources of uncertainties.

5. CONCLUSION

Using a silicon vertex detector, which was the largest operating at that time, we have isolated clean samples of charmed-particle decays and obtained accurate measurements of their lifetimes. We have measured the lifetimes of the different charmed mesons and of the Λ_c^+ baryon with the same experimental set-up, thus confirming the hierarchy in lifetimes already observed for these particles [7].

REFERENCES

[1] P. Astbury et al., Phys. Lett. **152B** (1985) 419.
E. Augé et al., Phys. Lett. **168B** (1986) 163 and **182B** (1986) 409.
R. Barate et al., Phys. Lett. **174B** (1986) 458; Z. Phys. **C33** (1987) 505.

[2] R. Barate et al., Nucl. Instrum. Methods **A235** (1985) 235.

[3] G. Barber et al., Nucl. Instrum. Methods **A253** (1987) 530.

[4] M. Koratzinos, Ph.D. thesis (Blackett Lab., Imperial College, Univ. of London), to be published.

[5] M.P. Alvarez et al. (NA14/2 Collab.), Measurement of D_s^+ and Cabibbo-suppressed D^+ decays, in preparation.

[6] M.P. Alvarez et al. (NA14/2 Collab.), Photoproduction of the Λ_c charmed baryon, in preparation.

[7] Particle Data Group, Phys. Lett. **B204** (1988) 1.

Table 1
Event samples used for lifetime measurements

Channel	Event sample	Selection cut	No. of signal candidates	No. of background candidates
$D^+ \to K^- \pi^+ \pi^+$	DP	8σ	200	130
$D^0 \to K^- \pi^+$	DP	4σ	250	300
$D^0 \to K^- \pi^+$	MF	4σ	360	190
$D^0 \to K^- \pi^+ \pi^+ \pi^-$	MF	6σ	280	210
$D_s^+ \to \phi \pi^+$	KF	$\Delta x > 1.5$ mm	15	3
$\Lambda_c \to pK^- \pi^+$	PF	$t > t^{min}$ a)	29	15

The samples of events used in this analysis are designated
DP: directly processed data through the CERN 3081E emulator 'farm'
MF: data extracted using the microstrip filter
KF: data extracted using the K^+K^- filter
PF: data extracted using the Kp filter

a) t^{min} corresponds to a minimum proper time of 0.22 ps or also to 3σ, because these events have been extracted from two independent analyses and merged to get the final data sample.

Table 2
Lifetime analysis of the samples of Table 1 (in ps)

Channel	Data sample	Measured lifetime	Statistical accuracy	Sources of systematic uncertainties					
				Total	Event reconstruction	Background level	Background shape	Acceptance correction	Feedthrough from other channels
$D^+ \to K^- \pi^+ \pi^+$	DP	1.03	$\pm$ 0.08	$\pm$ 0.06	$\pm$ 0.03	$\pm$ 0.03	$\pm$ 0.02	$\pm$ 0.03	-
$D^0 \to K^- \pi^+$	DP	0.436	$\pm$ 0.034	$\pm$ 0.03	$\pm$ 0.015	$\pm$ 0.015	$\pm$ 0.015	-	-
$D^0 \to K^- \pi^+$	MF	0.406	$\pm$ 0.029	$\pm$ 0.02	$\pm$ 0.015	$\pm$ 0.004	$\pm$ 0.01	$\pm$ 0.01	-
$D^0 \to K^- \pi^+ \pi^+ \pi^-$	MF	0.420	$\pm$ 0.028	$\pm$ 0.02	$\pm$ 0.015	$\pm$ 0.004	$\pm$ 0.01	$\pm$ 0.01	-
Combined D^0		0.417	$\pm$ 0.018	$\pm$ 0.015					
$D_s^+ \to \phi \pi^+$	KF	0.33	$+0.12$ -0.08	$\pm$ 0.03	$\pm$ 0.03	$\pm$ 0.01	$\pm$ 0.005	-	< 0.01
$\Lambda_c^+ \to pK^- \pi^+$	PF	0.18	$\pm$ 0.03	$\pm$ 0.03	$\pm$ 0.03	-	-	-	< 0.01

Figure captions

Fig. 1: The NA14/2 spectrometer.

Fig. 2: The vertex detector.

Fig. 3: $K^-\pi^+\pi^+$ mass distributions from data processed through the 3081 emulators:

a) with no cut on the separation of primary and secondary vertices,

b) with an $N_\sigma > 6$ cut on the vertex separation.

Fig. 4: Trigger conditions.

Fig. 5: D^+ lifetime measurement using the $K^-\pi^+\pi^+$ decay channel (DP sample):

a) $K^-\pi^+\pi^+$ invariant mass ($N_\sigma > 8$),

b) Proper-time distribution.

In this figure, and in all the following ones, the full line curve corresponds to the fitted distribution on all events in the mass region of the signal. The dashed curve gives the contribution to the previous distribution of events from the background.

Fig. 6: D^0 lifetime measurement using the $K^-\pi^+$ decay channel (MF sample):

a) $K^-\pi^+$ invariant mass ($N_\sigma > 4$),

b) Proper-time distribution.

Fig. 7: D^0 lifetime measurement using the $K^-\pi^+\pi^+\pi^-$ decay channel (MF sample):

a) $K^-\pi^+\pi^+\pi^-$ invariant mass ($N_\sigma > 6$),

b) Proper-time distribution.

Fig. 8: D_s^+ lifetime measurement using the $\phi\pi^+$ decay channel (KF sample):

a) $\phi\pi^+$ invariant mass ($\Delta_x > 1.5$ mm),

b) Proper-time distribution.

Fig. 9: Λ_c^+ lifetime measurement using the $pK^-\pi^+$ decay channel (PF sample):

a) $pK^-\pi^+$ invariant mass ($\tau > 0.22$ ps),

b) Proper-time distribution.

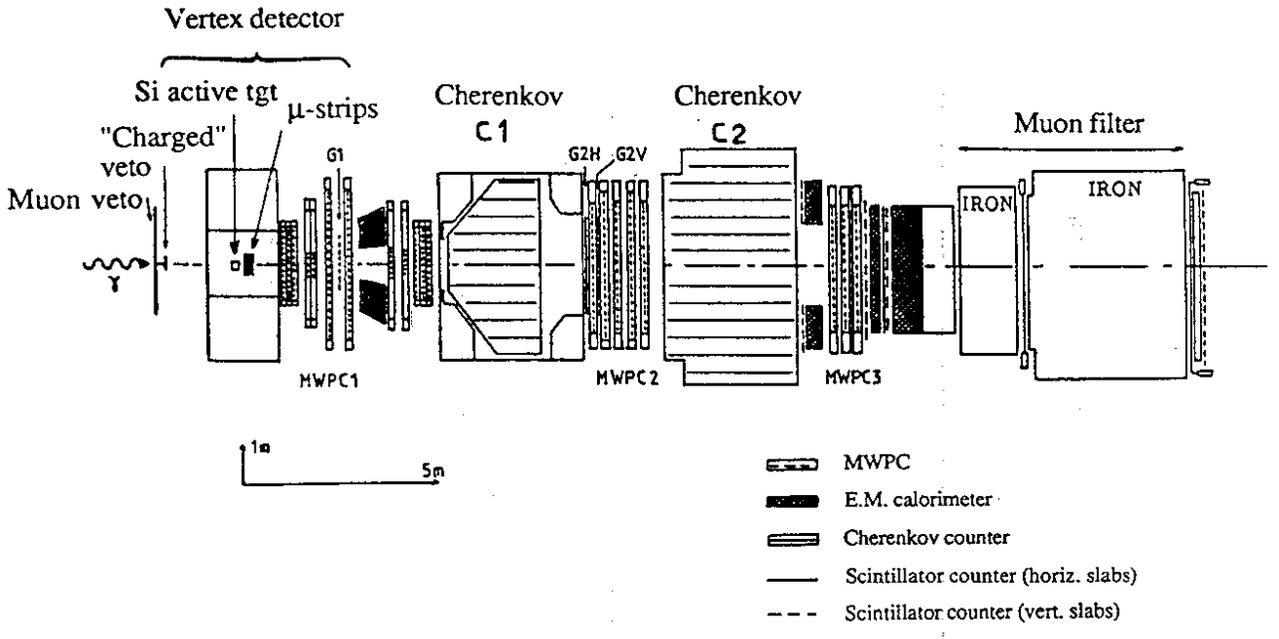
Vertex detector
Si active tgt
μ-strips
"Charged"
veto
Muon veto
γ
G1
Cherenkov
C1
G2H
G2V
Cherenkov
C2
Muon filter
IRON
IRON
MWPC1
MWPC2
MWPC3
1m
5m
MWPC
E.M. calorimeter
Cherenkov counter
Scintillator counter (horiz. slabs)
Scintillator counter (vert. slabs)

Fig. 1

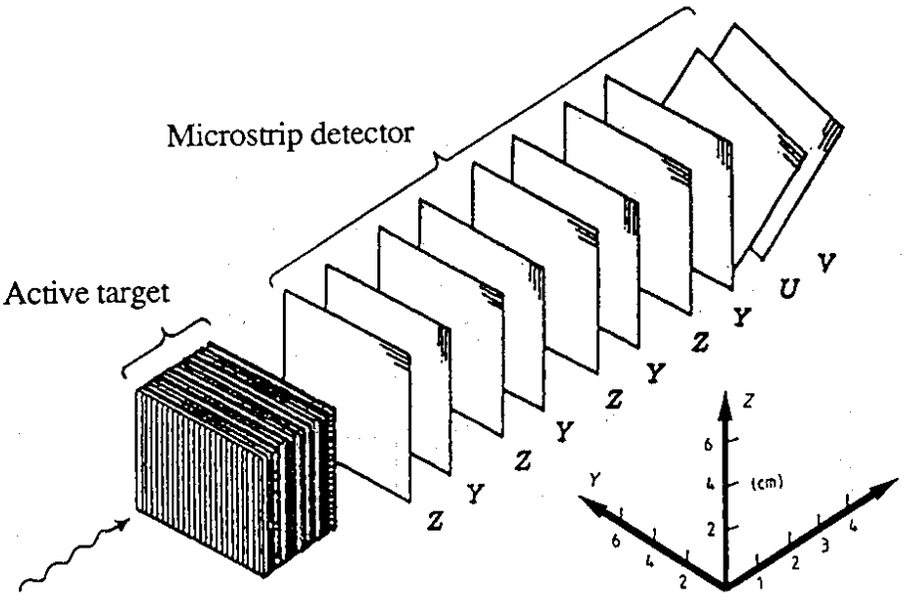
Microstrip detector
Active target
Z
Y
Z
Y
Z
Y
Z
Y
U
V
Z
(cm)
Y

Fig. 2

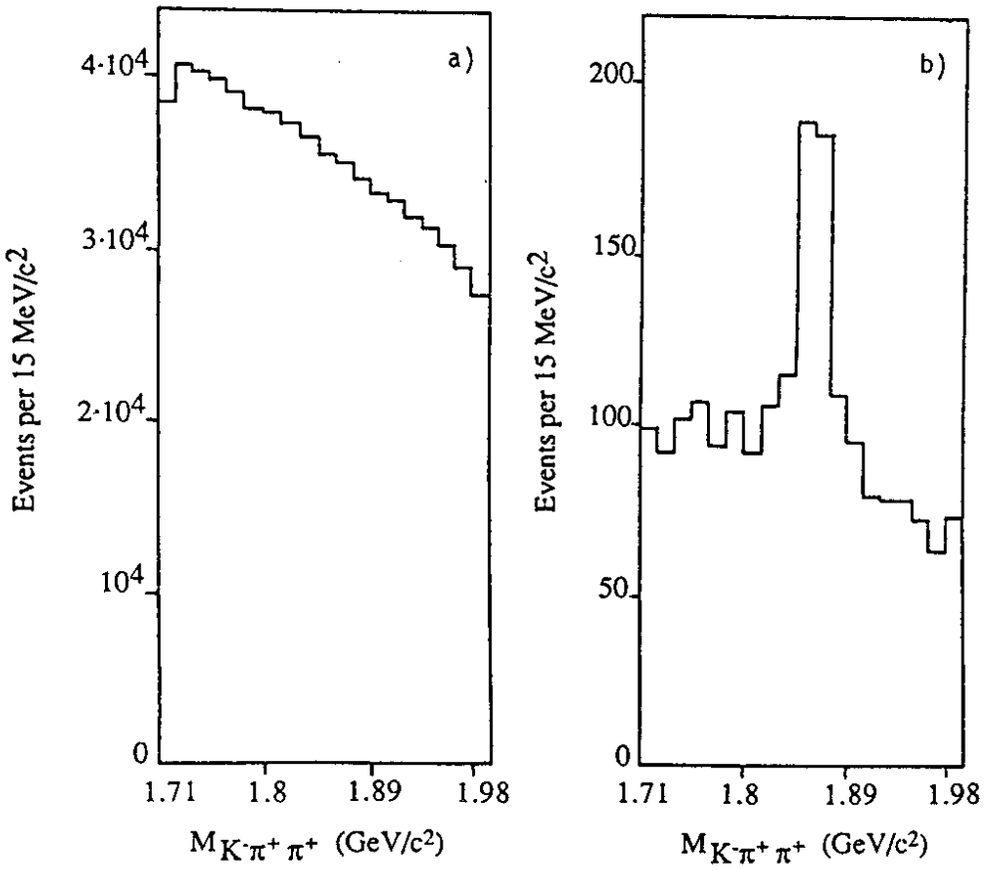
a)
b)
Events per 15 MeV/c2
4·10^4
3·10^4
2·10^4
10^4
0
200
150
100
50
1.71
1.8
1.89
1.98
M K-π+ π+ (GeV/c2)

Fig. 3

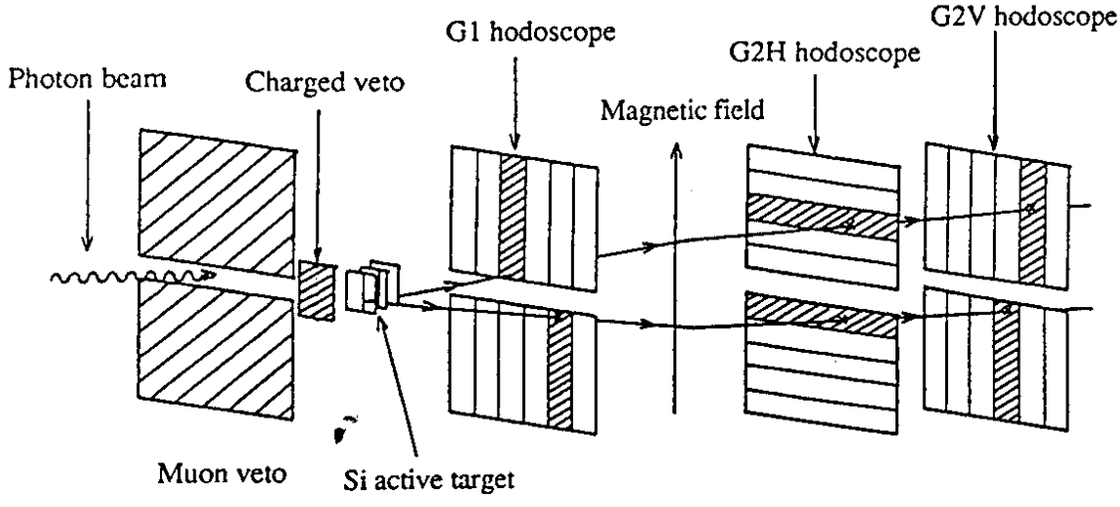
Photon beam
Charged veto
G1 hodoscope
Magnetic field
G2H hodoscope
G2V hodoscope
Muon veto
Si active target

Fig. 4

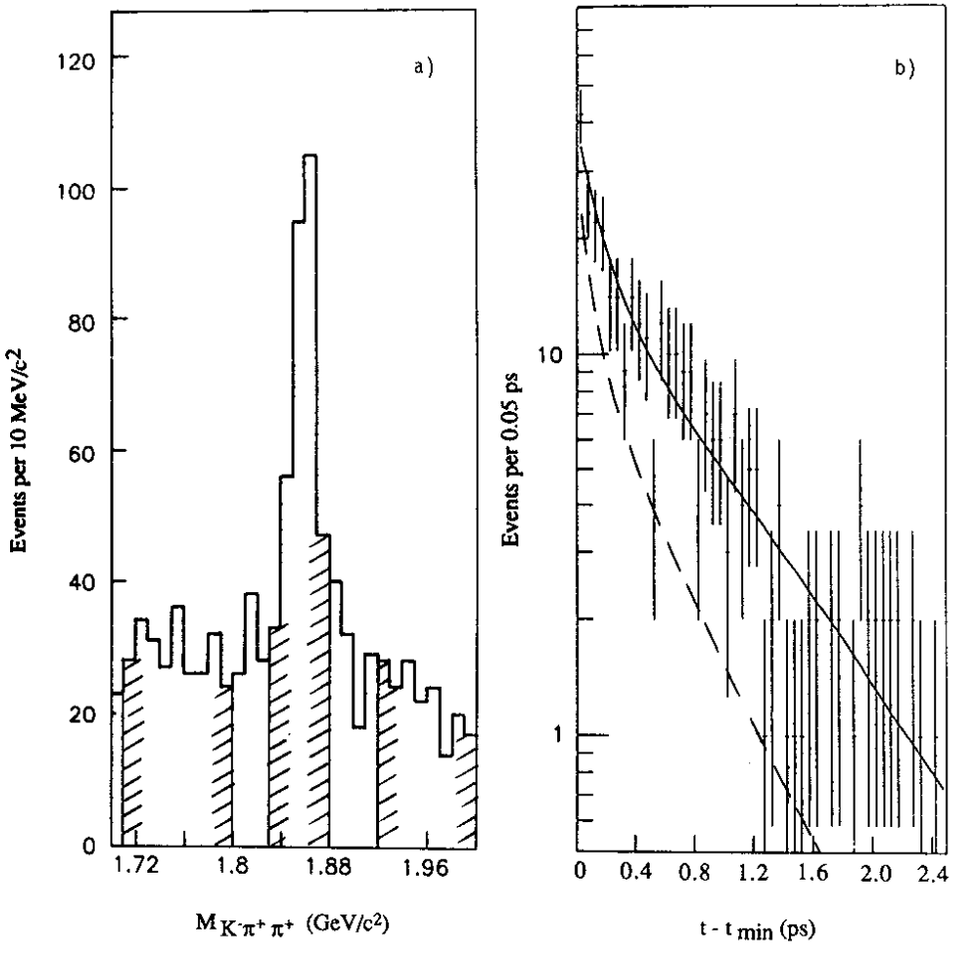
a)
b)
Events per 10 MeV/c2
Events per 0.05 ps
120
100
80
60
40
20
0
10
1
1.72
1.8
1.88
1.96
0
0.4
0.8
1.2
1.6
2.0
2.4
MK-π+ π+ (GeV/c2)
t - t min (ps)

Fig. 5

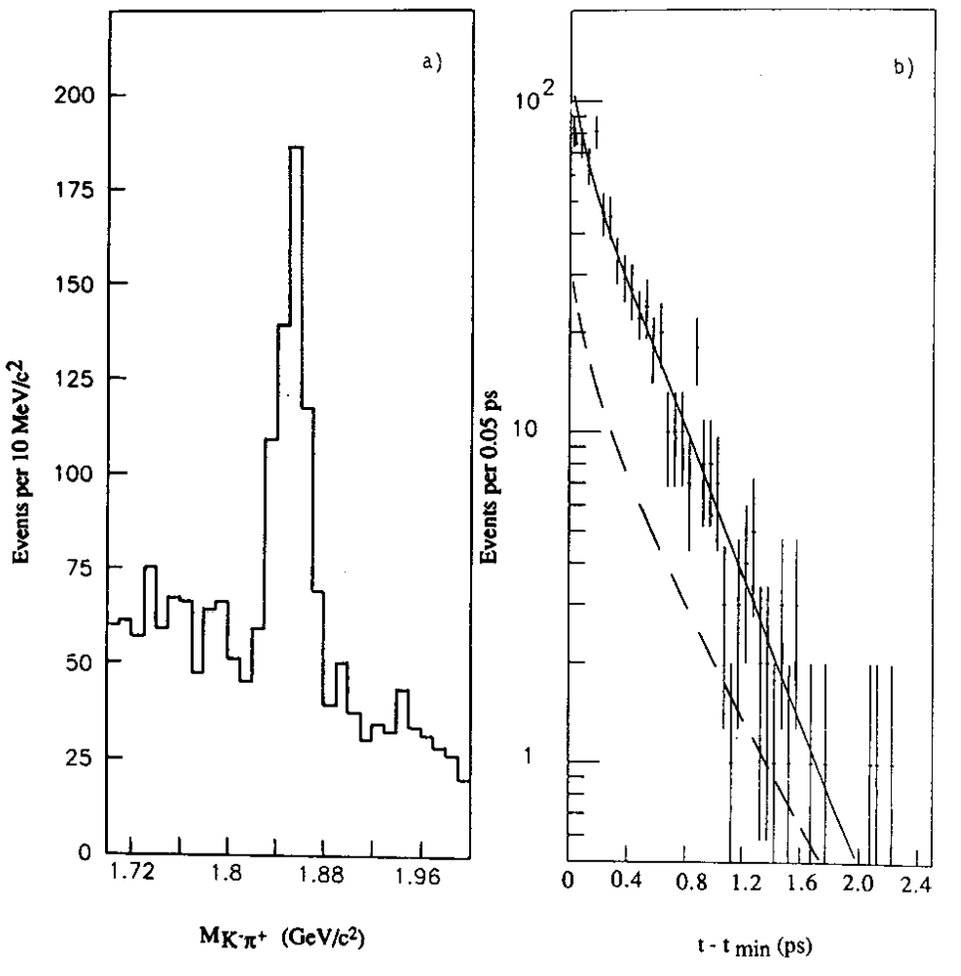
a)
b)
Events per 10 MeV/c2
Events per 0.05 ps
200
175
150
125
100
75
50
25
0
10
1
1.72
1.8
1.88
1.96
0
0.4
0.8
1.2
1.6
2.0
2.4
MK-π+ (GeV/c2)
t - t min (ps)

Fig. 6

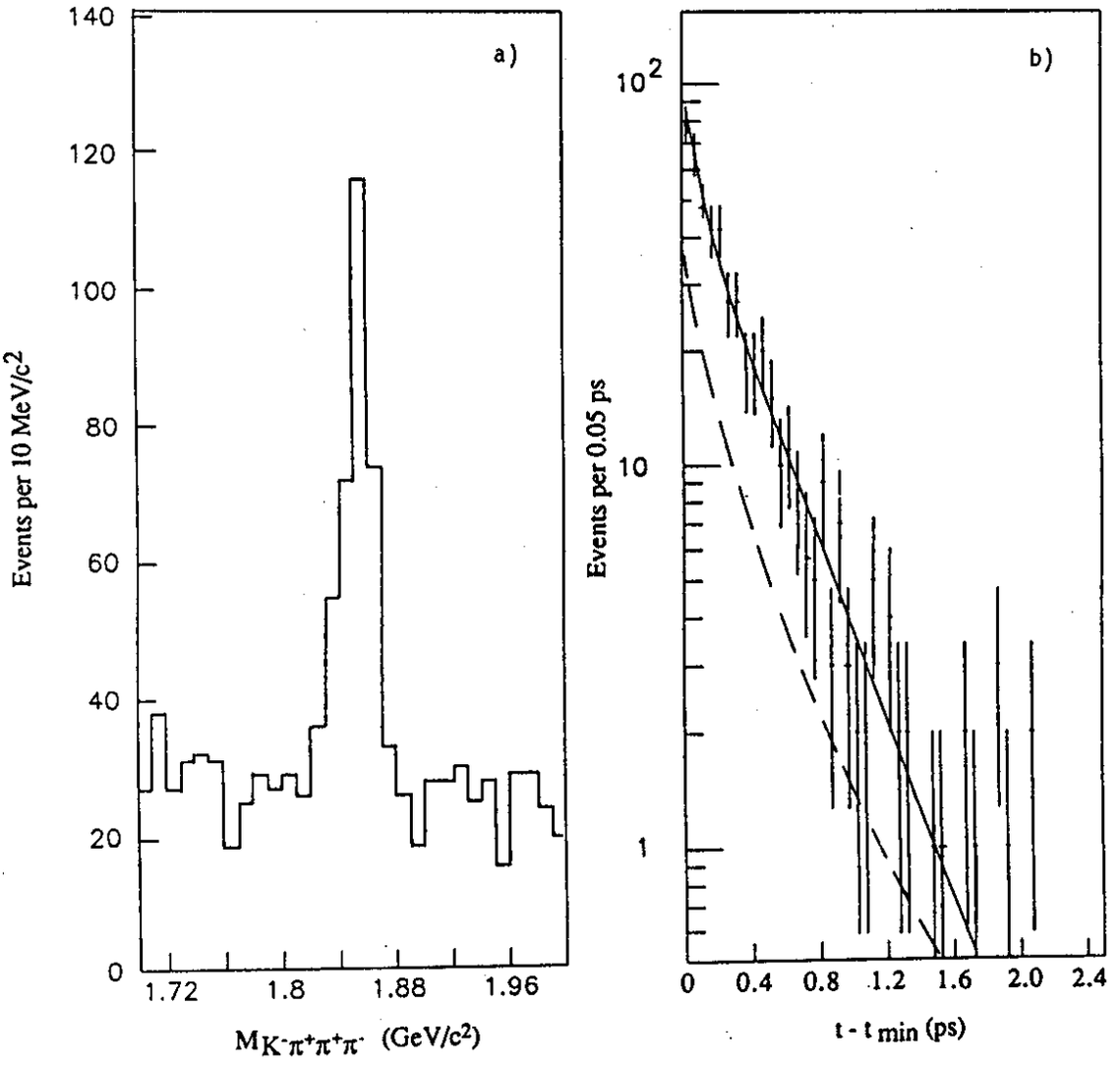
a)
b)
Events per 10 MeV/c2
Events per 0.05 ps
$M_{K^-\pi^+\pi^+\pi^-}$ (GeV/c2)
t - t min (ps)
140
120
100
80
60
40
20
0
10^2
10
1
1.72
1.8
1.88
1.96
0
0.4
0.8
1.2
1.6
2.0
2.4

Fig. 7

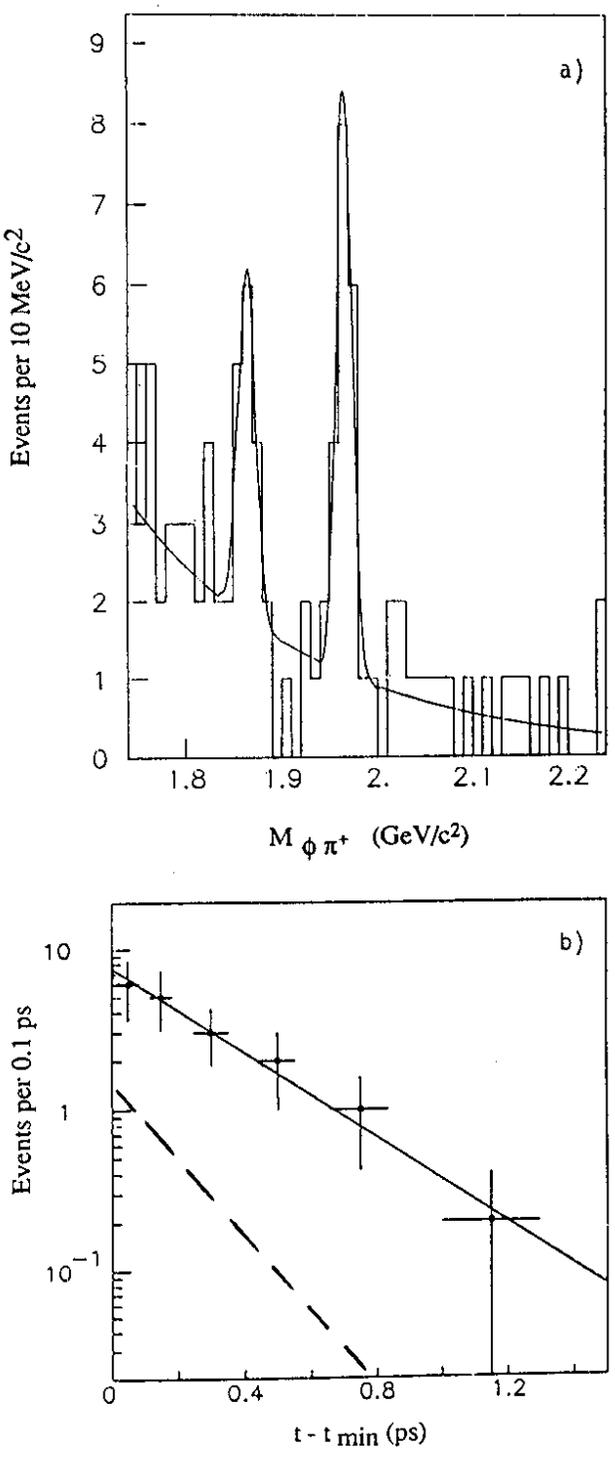
a)
Events per 10 MeV/c2
M φ π+ (GeV/c2)
b)
Events per 0.1 ps
t - t min (ps)

Fig. 8

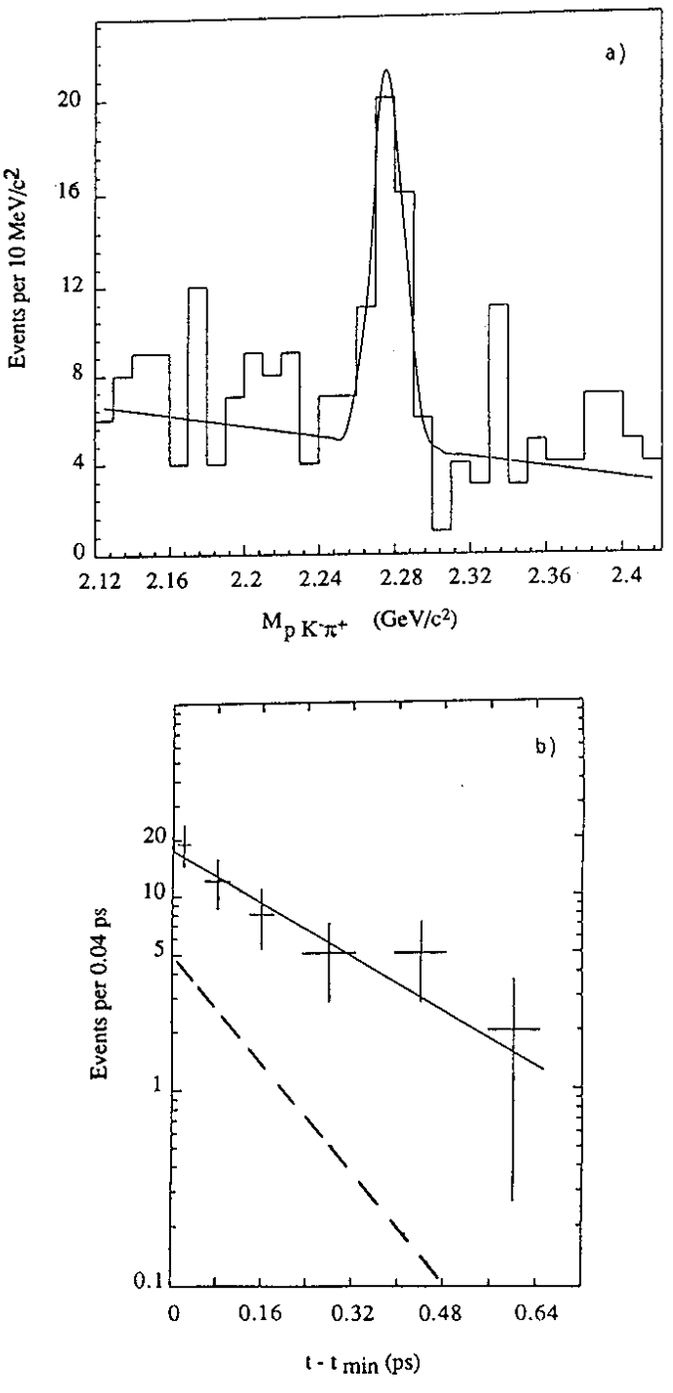
a)
Events per 10 MeV/c2
M p K-π+ (GeV/c2)
b)
Events per 0.04 ps
t - t min (ps)

Fig. 9